



# LAMINAR NATURAL CONVECTION OF BINGHAM FLUIDS IN A TRAPEZOIDAL ENCLOSURE HEATED FROM THE BOTTOM

Saleh Alshaaili<sup>1</sup>, Sean P. Malkeson<sup>2\*</sup>, Nilanjan Chakraborty<sup>1</sup>

<sup>1</sup>School of Engineering, Newcastle University, Newcastle-Upon-Tyne, NE1 7RU, United Kingdom

<sup>2</sup>School of Engineering, Liverpool John Moores University, Liverpool, L3 3AF, United Kingdom

## ABSTRACT

Laminar, steady-state, natural convection of Bingham fluids in trapezoidal enclosures with a heated bottom wall, adiabatic top wall and cooled inclined sidewalls has been analysed based on numerical simulations for a range of different values of nominal Rayleigh numbers (i.e.  $10^3 \leq Ra \leq 10^5$ ), Bingham numbers (i.e.  $0 \leq Bn \leq 0.5$ ), and inclination angles (i.e.  $30^\circ \leq \varphi \leq 60^\circ$ ) for a representative nominal Prandtl number (i.e.  $Pr = 10^3$ ). To conduct the parametric investigation, a commercial finite-volume solver has been used. It has been found that the mean Nusselt number  $\overline{Nu}$  increases with increasing  $Ra$  due to the strengthening of advective transport. However, an increase in the sidewall inclination  $\varphi$  leads to a decrease in  $\overline{Nu}$ . The value of  $\overline{Nu}$  was found to decrease with increasing  $Bn$ . At high values of  $Bn$ , fluid flow essentially ceases within the enclosure and the heat transfer takes place predominantly due to conduction and, therefore, the value of  $\overline{Nu}$  settles to a constant value, for a given value of  $\varphi$ , irrespective of the value of nominal  $Ra$ . Furthermore, an expression for the mean Nusselt number  $\overline{Nu}$  in a trapezoidal enclosure with heat bottom wall, cooled inclined sidewalls, and an adiabatic top wall accounting for the considered range of Rayleigh numbers  $Ra$ , Bingham numbers  $Bn$  and inclined wall angles  $\varphi$  has been identified which provides adequate approximation of the corresponding value obtained from the simulation.

## 1. INTRODUCTION

A yield stress fluid is a special type of non-Newtonian fluid which acts as a solid below a threshold stress (i.e., a yield stress  $\tau_y$ ) but flows like a fluid above this critical stress [1]. The use of yield stress fluids in industrial applications is wide-ranging with applications in nuclear waste cooling, food and chemical processing as well as cryogenic storage. The rheological behaviour of yield stress fluids is often modelled by a Bingham model which provides a linear strain rate dependence of the shear stress. The analysis of heat transfer in Bingham fluids is, therefore, one of practical interest but also of academic interest. The study of Bingham fluids has been considered for square enclosures [2], offering correlations for the mean Nusselt number  $\overline{Nu}$ . However, relatively limited attention has been directed to the natural convection of yield stress fluids in non-rectangular enclosures. The Rayleigh–Bénard convection (i.e., heated bottom wall and cooled top wall with adiabatic inclined side walls) within trapezoidal enclosures filled with viscoplastic fluid has been analysed by Aghighi et al. [3] across a range of parameters (i.e. the angle of inclination of the side walls  $\varphi$ , Rayleigh number  $Ra$  and Prandtl number  $Pr$ ). However, to the best of the authors' knowledge, the natural convection in Bingham fluids in a trapezoidal enclosure with heat bottom wall, cooled inclined sidewalls and an adiabatic top wall is yet to be considered in detail. Therefore, the objectives of the current study are, as follows:

1. To investigate the influence of the geometry of a trapezoidal cavity, Rayleigh number  $Ra$  and Bingham number  $Bn$  on the natural convection behaviour in Bingham fluids in a trapezoidal enclosure with heat bottom wall, cooled inclined sidewalls, and an adiabatic top wall.
2. To identify an expression for the mean Nusselt number  $\overline{Nu}$  in the considered configuration across the range of  $Ra$ ,  $Bn$  and  $\varphi$  examined.

\*Corresponding Author: [s.p.malkeson@ljmu.ac.uk](mailto:s.p.malkeson@ljmu.ac.uk)

## 2. MATHEMATICAL BACKGROUND & NUMERICAL IMPLEMENTATION

The schematic of the configuration considered in the current analysis is provided in Fig. 1a where  $L$  is the length of the bottom heated wall,  $H$  is the height of the trapezium and  $\varphi$  is the angle of inclination of the sidewall. The heated bottom wall is kept at a temperature  $T_H$  and the two inclined sidewalls are kept at a temperature  $T_C$ . It is assumed that  $T_H > T_C$ . The top wall is considered to be adiabatic in nature. The no-slip condition is applied to all walls. The flow is assumed to be laminar, incompressible, steady, and two-dimensional (i.e., the physical flow domain is assumed to be an infinitely long channel and, therefore, the third dimension is considered not to affect the flow field). The conservation equations for mass, momentum, and energy take the following form for the current study:

$$\partial u_i / \partial x_i = 0 \quad (1i)$$

$$\rho u_j (\partial u_i / \partial x_j) = -(\partial p / \partial x_i) + \delta_{2i} \rho g \beta (T_H - T_C) + \partial \tau_{ij} / \partial x_j \quad (1ii)$$

$$\rho u_j C (\partial T / \partial x_j) = k (\partial^2 T / \partial x_j \partial x_j) \quad (1iii)$$

where  $u_i(x_i)$  is the  $i^{th}$  component of velocity (spatial coordinate),  $\rho$  is the density,  $p$  is the pressure,  $g$  is the acceleration due to gravity,  $\beta$  is the thermal expansion coefficient,  $\tau_{ij}$  is the stress tensor,  $C$  is the specific heat,  $T$  is the temperature and  $k$  is the thermal conductivity. In Eq. 1ii, the Kronecker delta  $\delta_{2i}$  is employed to ensure that the buoyancy effect only occurs in the vertical direction (i.e.,  $x_2$  direction). The Bingham model for yield stress fluids can be expressed as [2]:

$$\underline{\underline{\dot{\gamma}}} = 0 \quad \text{for } \tau \leq \tau_y \quad (2i)$$

$$\underline{\underline{\tau}} = (\mu + \tau_y / \dot{\gamma}) \dot{\gamma}_{ij} \quad \text{for } \tau > \tau_y \quad (2ii)$$

where the components of the strain rate tensor  $\dot{\gamma}$  are given by:  $\dot{\gamma}_{ij} = \partial u_i / \partial x_j + \partial u_j / \partial x_i$ . In Eq. 2,  $\tau = [0.5 (\underline{\underline{\tau}} : \underline{\underline{\tau}})]^{0.5}$  and  $\dot{\gamma} = [0.5 (\underline{\underline{\dot{\gamma}}} : \underline{\underline{\dot{\gamma}}})]^{0.5}$ . The stress-shear rate characteristics of a Bingham fluid is approximated here by the bi-viscosity regularisation [4]:

$$\underline{\underline{\tau}} = \mu_{yield} \underline{\underline{\dot{\gamma}}} \quad \text{for } \dot{\gamma} \leq \tau_y / \mu_{yield} \quad (3i)$$

$$\underline{\underline{\tau}} = \tau_y (\dot{\gamma} / \dot{\gamma}) + \mu \dot{\gamma} \quad \text{for } \dot{\gamma} > \tau_y / \mu_{yield} \quad (3ii)$$

where  $\mu_{yield}$  is the yield viscosity and  $\mu$  is the plastic viscosity such that the solid material is represented by a high viscosity fluid [4]. A value of  $\mu_{yield} \geq 1000\mu$  satisfactorily mimics the true Bingham model according to its proponents [4], and here  $\mu_{yield} / \mu = 10^4$  is chosen to ensure the high-fidelity of the computational results. According to Buckingham's pi theorem, the Nusselt number  $Nu$  (defined as  $Nu = hL/k$  where  $h = q_w / (T_H - T_C)$  is the local heat transfer coefficient where  $q_w$  is the wall heat flux at the bottom hot wall) can be expressed in this configuration as  $Nu = f(Ra, Pr, H/L, \varphi, Bn)$  where the Bingham number  $Bn$ , Rayleigh number  $Ra$ , and Prandtl number  $Pr$  are defined as  $Ra = \rho g \beta \Delta T L^3 / (\mu \alpha)$ ,  $Bn = \tau_y L / (\mu \sqrt{g \beta \Delta T L})$  and  $Pr = C \mu / k$  where  $\Delta T = (T_H - T_C)$ , and  $\alpha = k / \rho C$  is the thermal diffusivity. The present analysis considers the aspect ratio  $H/L$  to be unity (i.e.,  $H/L = 1.0$ ).

A finite-volume (i.e., ANSYS-FLUENT) solver [5] has been used for solving the governing equations. A second-order upwind scheme (second-order central difference) has been used for the discretisation of convective (diffusive) terms. The coupling of velocity and pressure components is achieved using the SIMPLE (Semi-Implicit Method for Pressure-Linked Equations) algorithm [5], where the convergence criteria were set to  $10^{-6}$  for all relative (scaled) residuals. The boundary

conditions are:  $T = T_H$ ,  $u_1 = u_2 = 0$  at the bottom wall;  $T = T_C$ ,  $u_1 = u_2 = 0$  at the sidewalls and  $\partial T/\partial y = 0$ ,  $u_1 = u_2 = 0$  at the top wall. The parameters considered in the current study are:  $Ra = 10^3, 10^4, 10^5$ ;  $0 \leq Bn \leq 0.5$ ; and  $\varphi = 30^\circ, 45^\circ, 60^\circ$ . The Prandtl number  $Pr = 10^3$  was considered for all cases. A mesh independence analysis has been completed and a non-uniform unstructured triangular mesh of 22500 cells (shown in Fig. 1b) is used for the study. This mesh provides agreement of  $Nu$  on the hot wall to within 2% with a mesh of 30625 cells but with a 26% reduction in computational cost, giving balance between accuracy and cost for the parametric investigation where 80 simulations were considered. Figure 1b also provides the non-dimensional temperature  $\theta = (T - T_C)/(T_H - T_C)$  field of an example case (i.e.,  $Ra = 10^3$ ,  $Bn = 0.5$ ,  $\varphi = 30^\circ$ ). Furthermore, the currently considered numerical implementations have been tested against benchmarks with the natural convection of Newtonian fluids in a square enclosure (i.e.,  $\varphi = 0^\circ$ ) with differentially heated sides [2] and natural convection heat transfer in partially divided trapezoidal cavities [6]. For both benchmark studies, satisfactory agreements (i.e., typically within 0.5% but, at most, 2% across all benchmark cases considered) were obtained.

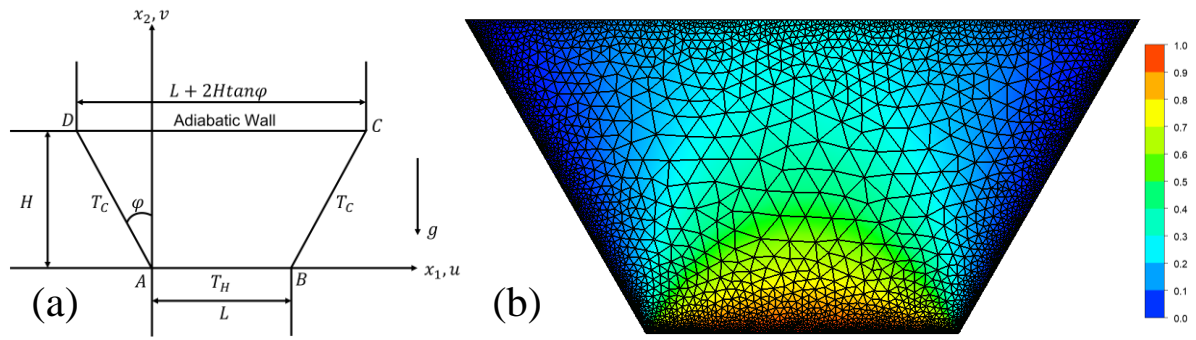


**Figure 1:** (a) Schematic of considered configuration, and (b) the non-dimensional temperature  $\theta = (T - T_C)/(T_H - T_C)$  field for the  $Ra = 10^3$ ,  $Bn = 0.5$ ,  $\varphi = 30^\circ$  case with the mesh superimposed.

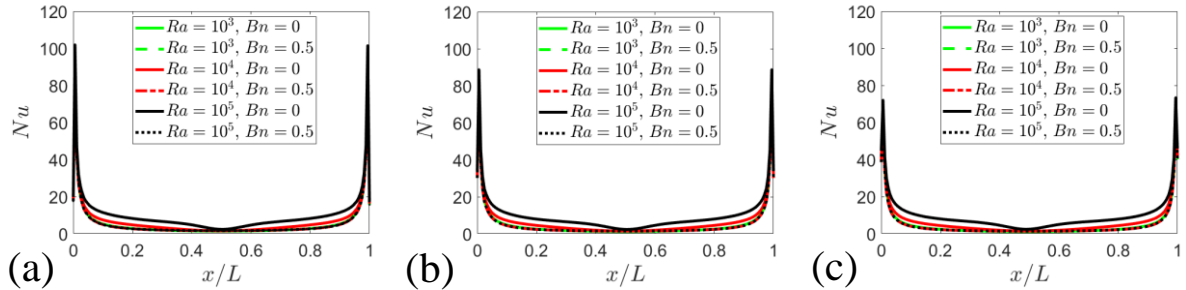


**Figure 2:** The variations of local Nusselt number  $Nu$  on the hot bottom wall with normalised horizontal distance  $x_1/L$  for (a)  $Ra = 10^3$ ,  $Ra = 10^4$  and  $Ra = 10^5$  where  $Bn = 0.5$ ,  $Pr = 10^3$  compared to the corresponding Newtonian fluid for (a)  $\varphi = 30^\circ$ , (b)  $\varphi = 45^\circ$  and (c)  $\varphi = 60^\circ$  configurations.

### 3. RESULTS & DISCUSSION

In the following sections, the effects of  $Ra$ ,  $Bn$ , and  $\varphi$  on the heat transfer behaviour in the trapezoidal enclosure are discussed. The variations of the local Nusselt number  $Nu$  on the hot wall with normalised horizontal distance  $x_1/L$  for  $Ra = 10^3$ ,  $10^4$  and  $10^5$  where  $Bn = 0.5$ ,  $Pr = 10^3$ , in comparison to the corresponding Newtonian fluid (i.e.  $Bn = 0$  where the yield stress  $\tau_y = 0$ ), are shown for  $\varphi = 30^\circ$ ,  $\varphi = 45^\circ$ , and  $\varphi = 60^\circ$  in Figs. 2a-c, respectively. Figures 2a-c show that  $Nu$  increases with increasing  $Ra$  for both the Bingham and Newtonian fluids considered. Furthermore, Figs. 2a-c show that the values of  $Nu$  are generally greater for the Newtonian fluid than the Bingham fluid across  $x_1/L$  with the same nominal  $Ra$ . This difference is most apparent in  $Ra = 10^5$  cases and is due to the

strengthening of buoyancy effects with increasing  $Ra$  which will have the greatest effect in the  $Bn = 0$  cases where there is yield stress  $\tau_y = 0$ . Figures 3a-f show the contours of non-dimensional temperature  $\theta$  for Bingham fluids of  $Bn = 0.5$  (i.e., top row) and the corresponding Newtonian fluid (i.e., bottom row) for  $Ra = 10^3, 10^4$  and  $10^5$  where  $Pr = 10^3$  and  $\varphi = 30^\circ$ . Figures 3d-f show that there are significant changes in the behaviour of  $\theta$  with increasing  $Ra$  for Newtonian fluids. However, Figs. 3a-c show that for Bingham fluids the contours of  $\theta$  show negligible variation with increasing  $Ra$  for  $Bn = 0.5$ . This suggests that for sufficiently large values of  $Bn$ , conduction begins to play the dominant role in thermal transport and the nominal Rayleigh number  $Ra$  no longer affects the value of  $Nu$ .

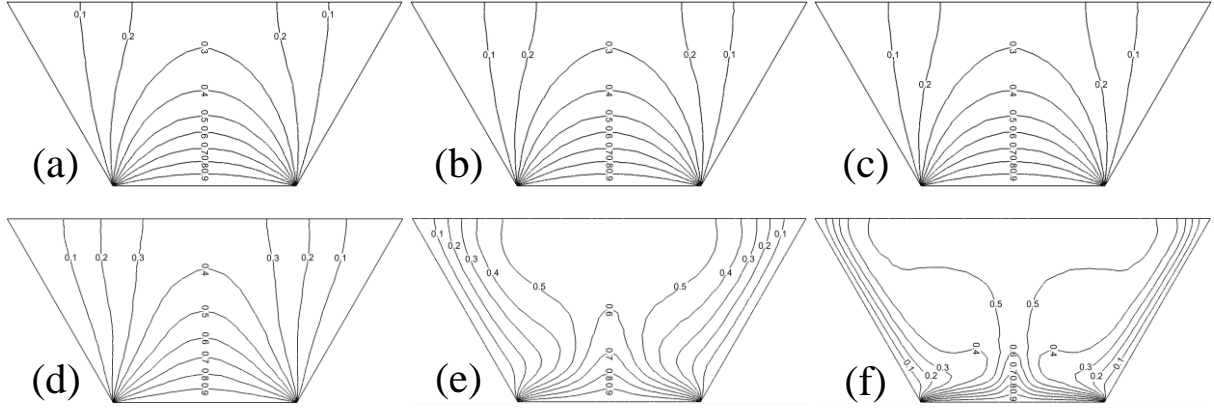


**Figure 3:** Contours of non-dimensional temperature  $\theta$  for  $Bn = 0.5$  (i.e., top row) and the corresponding Newtonian fluid (i.e., bottom row) for  $Ra = 10^3, 10^4$  and  $10^5$  where  $Pr = 10^3$  and  $\varphi = 30^\circ$ .

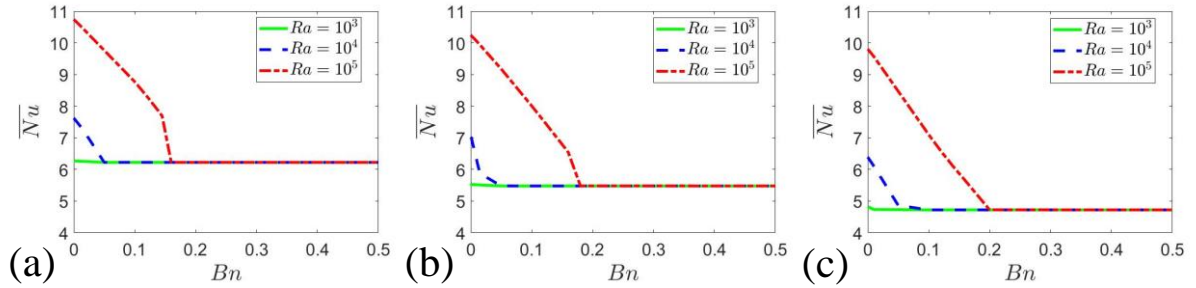


**Figure 4:** Variations of the mean Nusselt number  $\overline{Nu}$  on the hot bottom wall with Bingham number  $Bn$  for  $Ra = 10^3, 10^4$  and  $10^5$  where  $Pr = 10^3$  for (a)  $\varphi = 30^\circ$ , (b)  $\varphi = 45^\circ$ , and (c)  $\varphi = 60^\circ$ .

The effects of  $Bn$  on the nature of the heat and mass transfer in the trapezoidal cavity can further be shown through the variation of the mean Nusselt number  $\overline{Nu}$  with  $Bn$  as shown for  $Ra = 10^3, 10^4$  and  $10^5$  where  $Pr = 10^3$  for  $\varphi = 30^\circ, 45^\circ$  and  $60^\circ$  in Figs. 4a-c, respectively. Figures 4a-c show that, for a given set of values of  $Ra$  and  $\varphi$ ,  $\overline{Nu}$  is found to decrease as  $Bn$  increases until  $\overline{Nu}$  plateaus to a constant value (i.e., at  $Bn = Bn_{max}$ ) which, for a given  $\varphi$ , is common across all  $Ra$  considered. For larger values of  $Bn$ , where  $\tau_y$  is sufficiently large relative to the viscous stress, despite increases in  $Ra$ , no significant flow is induced within the enclosure and conduction heat transfer plays the dominant role as previously discussed. Importantly, however, Figs. 4a-c shows that an increase in  $Ra$  leads to an increase in  $\overline{Nu}$  for sufficiently low values of  $Bn$  where flow is induced, and convection heat transfer occurs. Moreover, for higher values of  $Ra$  where buoyancy forces are greater, the value of  $Bn$  at which  $\overline{Nu}$  settles to a constant value also increases. The effect of  $Bn$  on the flow behaviour within the enclosure can further be examined by considering the non-dimensional vertical velocity  $U_2 = u_2 L / \alpha$  at the vertical centreline (vertical line of symmetry) as shown for  $Ra = 10^5$  where  $Pr = 10^3$  for  $\varphi = 30^\circ$ , in Figs. 5a-c, respectively. Figures 5a-c show that  $U_2$  decreases with increasing  $Bn$ . This corroborates the observations from Figs. 4a-c which indicates that an increase in  $Bn$  suggests strengthening of flow resistance relative

to the buoyancy forces and it is reflected in a reduction in the non-dimensional vertical velocity  $U_2$ . As such, this suggests that a further increase in  $Bn$  will eventually lead to a negligible value of  $U_2$  where conduction will become the sole heat transfer mechanism.

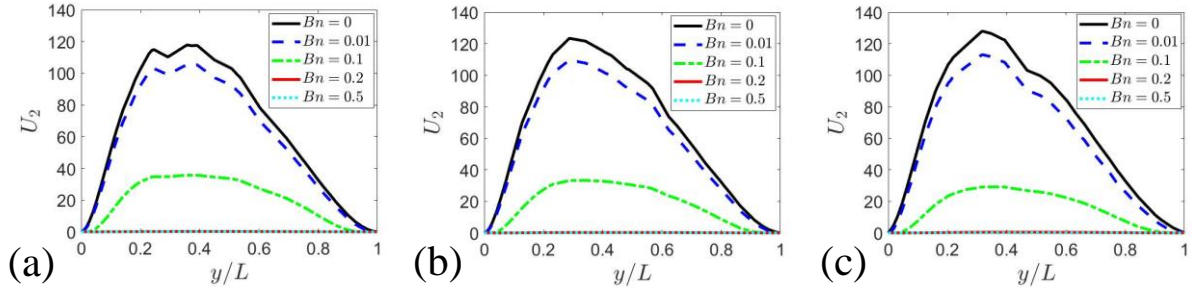


**Figure 5:** Variation of non-dimensional vertical velocity  $U_2 = u_2 L / \alpha$  along the vertical centreline for different Bingham numbers for  $Ra = 10^5$  and  $Pr = 10^3$  for (a)  $\varphi = 30^\circ$ , (b)  $\varphi = 45^\circ$ , and (c)  $\varphi = 60^\circ$ .

The effect of  $\varphi$  on the heat transfer behaviour can be gleaned by considering the variation of  $\overline{Nu}$  with  $Bn$  for  $\varphi = 30^\circ$ ,  $45^\circ$  and  $60^\circ$ , which is shown in Fig. 6. It is evident from Fig. 6 that an increase in the vertical angle  $\varphi$  leads to a decrease in  $\overline{Nu}$  which is due to the walls at temperature  $T_c$  (i.e., cold walls, inclined to the vertical) becoming longer leading to greater area for losing heat from the cavity and, therefore, a smaller amount of heat flux is needed for higher values of  $\varphi$  to maintain the same temperature difference  $\Delta T = (T_H - T_C)$ . The observed effects of  $Ra$ ,  $Bn$  and  $\varphi$  on the heat transfer behaviour must be accounted for when obtaining an expression for  $\overline{Nu}$ .

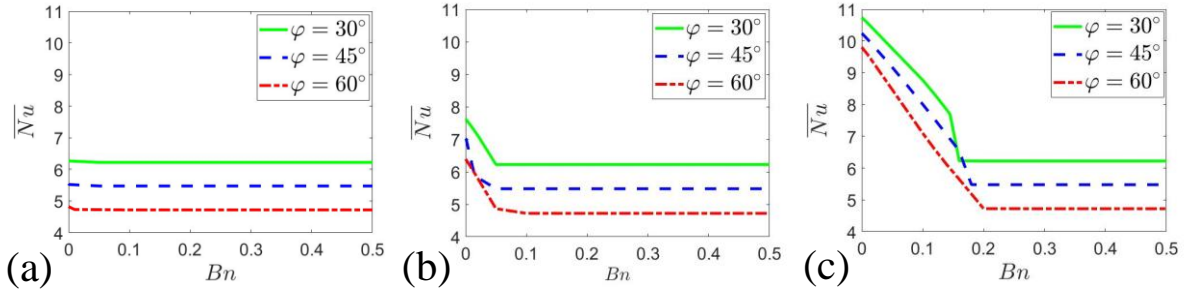


**Figure 6:** The variation of mean Nusselt number  $\overline{Nu}$  for the hot bottom wall with Bingham number  $Bn$  for  $\varphi = 30^\circ$ ,  $45^\circ$  and  $60^\circ$  where  $Pr = 10^3$  for (a)  $Ra = 10^3$ , (b)  $Ra = 10^4$ , and (c)  $Ra = 10^5$ .

Previous analyses have developed expressions for the mean Nusselt number  $\overline{Nu}$  for Bingham fluids in different enclosures across a range of  $Ra$ ,  $Pr$ ,  $Bn$  and, where appropriate, aspect ratios which have extended upon the expressions for Newtonian fluids [2,6,7]. Based on scaling arguments [6,7], an expression can be proposed which varies in the region of  $0 \leq Bn \leq Bn_{max}$  accounting for the fall in  $\overline{Nu}$  in this range and takes a constant value for  $Bn > Bn_{max}$ . As such, the following expression for  $\overline{Nu}$  can be proposed which extends expression for square enclosures for trapezoidal enclosures:

$$\overline{Nu} = 1 + \frac{ARa^{1/2}}{\left[ \frac{Bn+1}{2} \sqrt{Bn^2 + 4 \left( \frac{Ra}{Pr} \right)^{1/2}} \right]} \left[ 1 - \left( \frac{Bn}{Bn_{max}} \right)^{3/5} \right]^b \text{ for } Bn < Bn_{max}, \text{ and } \overline{Nu} = 1 \text{ for } Bn \geq Bn_{max} \quad (4)$$

where  $A = aC_{\varphi 1} Ra^{m-0.25} [Pr^{n-0.25} / (1 + Pr)^n] - 1 / (Ra^{0.25} Pr^{0.25})$ ,  $b = 0.025 Ra^{0.25} Pr^{0.25}$  with  $a = 0.178$ ,  $m = 0.269$ ,  $n = 0.02$  and  $C_{\varphi 1} = 0.5^{-\varphi[\text{rad}]}$  which causes Eq. 4 to revert back to the expression for square enclosures as  $\varphi$  tends to zero. The expression given in Eq. 4 is dependent upon the adequate representation of  $Bn_{max}$ . An expression for  $Bn_{max}$  which extends upon a previous

expression proposed for square enclosures [2,6] to application in trapezoidal enclosures such that  $Bn_{max} = (1 + C_{\varphi 2})[0.0019 \ln(Ra) - 0.0128]Ra^{0.55}Pr^{-0.50}$  where  $C_{\varphi 2} = 4\varphi[rad]/\pi[rad]$ . This expression for  $Bn_{max}$  tends back to the expression for square enclosures [2,6] as  $\varphi$  tends to zero. It is evident from Figs. 7a-c that the expression given by Eq. 4 generally provides satisfactory qualitative and mostly quantitative variation of  $\overline{Nu}$  for the range of  $Ra$ ,  $Bn$  and  $\varphi$  considered.

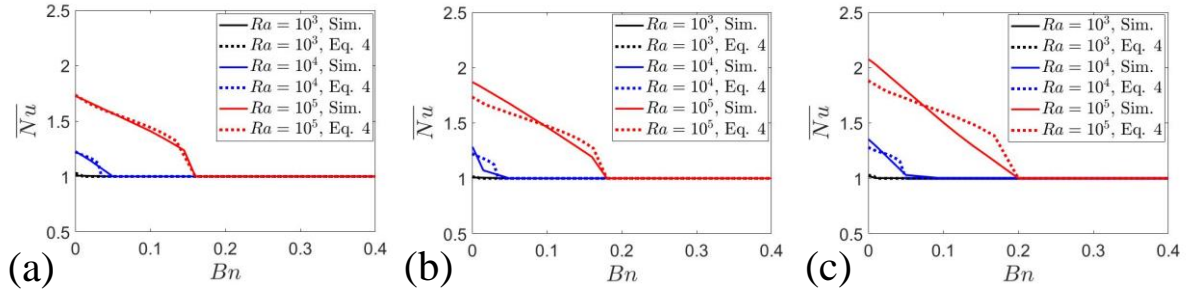


**Figure 7:** The variation of  $\overline{Nu}$  normalised by value at  $Bn_{max}$  with  $Bn$  for  $Ra = 10^3, 10^4$  and  $10^5$  where  $Pr = 10^3$  for (a)  $\varphi = 30^\circ$ , (b)  $\varphi = 45^\circ$ , and (c)  $\varphi = 60^\circ$  along with the values from Eq. 4.

#### 4. CONCLUSIONS

Laminar, steady-state, natural convection of Bingham fluids in trapezoidal enclosures with a heated bottom wall, adiabatic top and cooled inclined sidewalls has been analysed based on numerical simulations for a range of different values of  $Ra$  (i.e.,  $10^3 \leq Ra \leq 10^5$ ),  $Bn$  (i.e.,  $0.0 \leq Bn \leq 0.5$ ), and  $\varphi$  (i.e.,  $30^\circ \leq \varphi \leq 60^\circ$ ). It has been found that  $\overline{Nu}$  increases with increasing  $Ra$  due to the strengthening of advective transport. However, an increase in the sidewall inclination  $\varphi$  leads to a decrease in  $\overline{Nu}$ . The value of  $\overline{Nu}$  was found to decrease with increasing  $Bn$  value. At high values of  $Bn$ , the fluid flow becomes negligible within the enclosure and heat transfer begins to take place due to thermal conduction and, therefore, the value of  $\overline{Nu}$  settles to a constant value irrespective of the value of  $Ra$ . Furthermore, a correlation for  $\overline{Nu}$  for the considered configuration accounting for the range of  $Ra$ ,  $Bn$  and  $\varphi$  has been proposed which provides satisfactory predictions of the qualitative variation of  $\overline{Nu}$ .

#### REFERENCES

- [1] E.C. Bingham, An Investigation of the Laws of Plastic Flow. Bulletin of the Bureau of Standards, 13:2 (1916) 309–353.
- [2] O. Turan, N. Chakraborty, & R.J. Poole, Laminar natural convection of Bingham fluids in a square enclosure with differentially heated side walls. Journal of Non-Newtonian Fluid Mechanics, 165 (2010) 901-913.
- [2] M.S. Aghighi, A. Ammar, H. Masoumi & A. Lanjani, Rayleigh–Bénard convection of a viscoplastic liquid in a trapezoidal enclosure. International Journal of Mechanical Science, 180 (2020) 105630.
- [3] E.J. O’Donovan, & R.I. Tanner, Numerical study of the Bingham squeeze film problem. Journal of Non-Newtonian Fluid Mechanics, 15 (1984) 75-83.
- [4] ANSYS Fluent User's Guide, 2020R2.
- [5] F. Moukalled, & M. Darwish, Natural Convection in Partitioned Trapezoidal Cavity Heated from The side. Numerical Heat Transfer, Part A: Applications, 43:5 (2010) 543-563.
- [6] O. Turan, A. Sachdeva, R.J. Poole, & N. Chakraborty, Laminar Rayleigh–Bénard convection of yield stress fluids in a square enclosure, Journal of Non-Newtonian Fluid Mechanics, 172 (2012) 83–96.
- [7] S. Yigit, & N. Chakraborty, Influences of aspect ratio and wall boundary condition on laminar Rayleigh–Bénard convection of Bingham Fluids in rectangular enclosures. International Journal of Numerical Methods in Heat and Fluid Flow 27:2 (2017) 310-333.